NUMERICAL SIMULATION OF SUPERSONIC FLOWFIELD WITH SECONDARY INJECTION

R.S. Amano*, D. Sun*
***University of Wisconsin-Milwaukee**

Keywords: *Shock wave, supersonic flow, jet injection*

Abstract

Two and three-dimensional steady flowfields generated by transverse secondary injection into a supersonic flow, was simulated by solving the Favre-averaged Navier-Stokes equations using the weighted essentially nonoscillatory (WENO) schemes and the Jones-Launder $k-\varepsilon$ model. Both the two-dimensional and three-dimensional results are given. Some parameters affecting the penetration height and separation length of the interactive flowfield, including the total pressure ratio of the jet to the freestream, the boundary layer thickness, slot width, the Mach number of the freestream and injection, the jet angle, and the shape of the injection orifice in the 3D flowfield, were calculated in more detail.

1 Introduction

The mixing flowfield resulting from a gaseous injection injected transversely into a supersonic freestream is encountered in many fields, such as rocket motor thrust vector control systems, supersonic combustion, high-speed flight vehicle reaction control jets, and gas-turbine cooling systems [1-3]. The mixing flowfield is very complex, which includes bow shock wave, boundary layer separation, and vortexes. The 2-D and 3-D schematic of the transverse jet injected into a supersonic freestream appears in Figure 1. In the 3-D flowfield, a three-dimensional bow shock forms ahead of the injection and interacts with the approaching boundary layer, resulting in a separation bubble. A barrel shock also occurs as the under expanded jet accelerates into the freestream. Acceleration of the jet core flow continues until a normal shock, or Mach disk, forms. Directly downstream of the jet plume, another separated zone develops in the region between the jet exit and the boundary layer reattachment point. A pair of counter-rotating vortices generated within the jet fluid and the horseshoe vortex region also forms near the jet exit and wraps around the injector, as illustrated in the schematic. The structure of the 2-D flowfield is similar to the 3-D flowfield.

Zukoski and Spaid investigated the flowfields. They proposed an analytical method to predict the penetration height. In their studies, Mach number and static pressure of freestream, mass flow rate, stagnation temperature, and gas constant of the injection are the main control parameters. Schetz and Billig constructed the concept of "effective back pressure." They thought that the penetration height was controlled by the momentum flux ratio of jet to freestream. Orth and Funk studied the influence of momentum flux ratio, pressure, and Mach number of the injection. Their studies show that under a fixed momentum flux ratio, it is hard to increase the penetration height by the increasing jet pressure. Povinelli, Cohen and Strike obtained the experience an formulas to predict penetration height [4-6]. Povinelli and Strike's results are similar to Billig's results They all give the penetration height versus Mach number and the total pressure of the injection to certain pressure, which is "effective back pressure" in Billig's study, total pressure of freestream in Povinelli's and static pressure of freestream in Strike's study. In Cohen's model, the influence of the jet angle is considered. M. R. Gruber etc. studied the difference between circular and elliptical injection orifices[7]. Liscinsky and

True studied the influences of various jet orifices and arrangement forms [8]. Roger etc. used GASP version 3.0 to analyze the influence of different jet Mach numbers and different boundary layer thickness [9].

Our goal in this work was to find how some parameters, such as the total pressure ratio of jet to freestream, boundary layer thickness, width of the slot nozzle, Mach number, and jet angle, how to affect the penetration height and separation length.

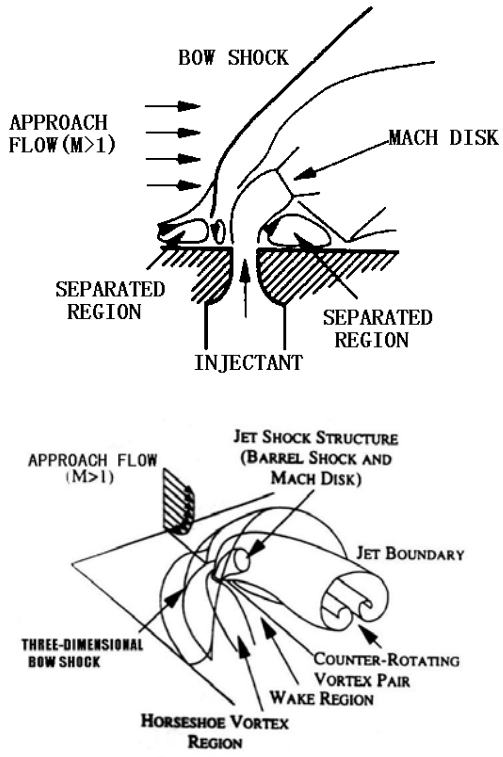

Figure 1. Schematic of 2D and 3D flowfield with secondary injection

2 Numerical Method

In our study, a third order WENO scheme and Runge-Kutta method [10] were used for spatial and temporal discretization to resolve the two and three dimensional Favre-averaged Navier-Stokes equations. The Jones-Launder low-Reynolds-number $k-\varepsilon$ turbulent model was used to simulate turbulent flow.

3 Results

3.1 Definition of penetration height and separation length

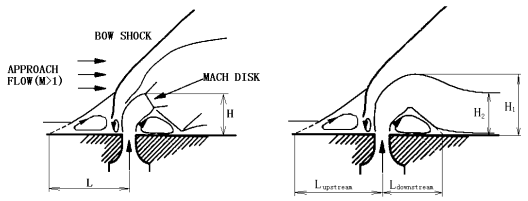

(a) (b)

Figure 2 Definition of penetration height and separation length.

Generally, separation lengths reflect the intensity of the bow shock wave and the extent of separation. Because there is flow separation downstream of the injection, we define two separation lengths, upstream separation length $L_{upstream}$ and downstream separation length $L_{downstream}$. The injection is nearly parallel with the freestream after it passes through the Mach disk. Since there is a little increase above Mach disk, we define two penetration heights in our study. One is the highest penetration height H_1, the other is the height at the downstream of the injection, H_2. The parameters affecting penetration height and separation length are discussed below.

3.2 Total pressure ratio of injection to freestream

Table 1 Calculation Condition

	Freestream (air)	Injection (air)
Mach number	3.71	1.0
Density	1	17.2958·k
Pressure	1/1.4	54.09·k
Velocity	3.71	1.7684
Temperature	1.0	3.1274

k = total pressure of injection / total pressure of freestream

The total pressure ratio of injection to freestream is a main parameter affecting the

flowfield. In our study, both the freestream and injection are air. When discussing total pressure ratio, the total temperatures of the freestream and injection and the total pressure of the freestream are fixed. The slot width is 1mm, and the Mach number of injection is 1. The boundary layer thickness at the inlet is 4.9mm. Table 1 shows the calculation condition.

The results, the penetration height and separation length versus the total pressure ratio, are shown in Figs. 3 and 4. We can see that the curves are almost linear. As the total pressure ratio of jet to freestream is low, the bow shock wave is weak and the penetration height is low. When increasing the total pressure ratio, the influence of the injection is extended. The penetration height and separation length are all increased, which reflects the stronger shock wave.

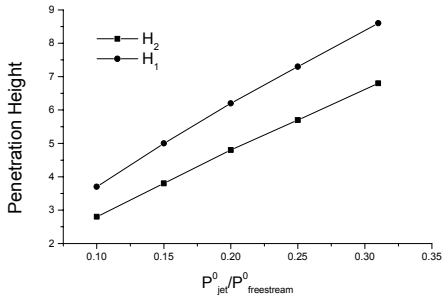

Fig. 3 Penetration height versus total pressure ratio

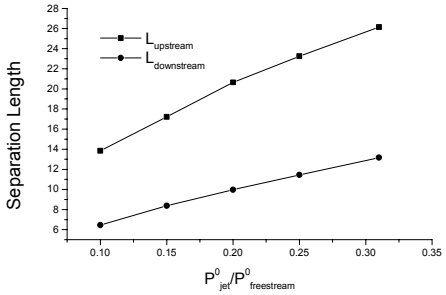

Fig. 4 Separation length versus total pressure ratio

3.3 Boundary layer thickness

Flow separation occurring in the boundary layer is induced by the interaction between the shock wave and boundary layer, so the change of boundary layer thickness must affect flow separation. The calculation is under the conditions of a freestream Mach number of 3.71, unit Reynolds number of $2.01\times10^7/m$, slot width of 1mm, jet Mach number of 1.0, and a total pressure ratio of 0.31. We calculated the flowfield under three boundary layer thicknesses, which were 1.8mm, 3.1mm, and 4.9mm.

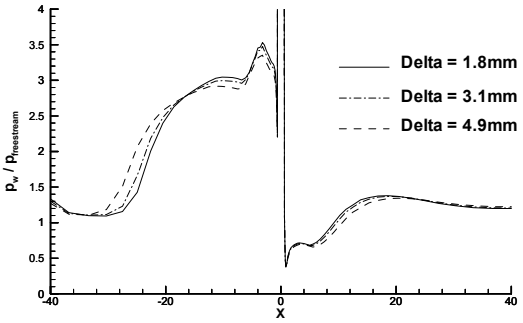

Fig. 5 Distribution of wall pressure under variable boundary layer thickness

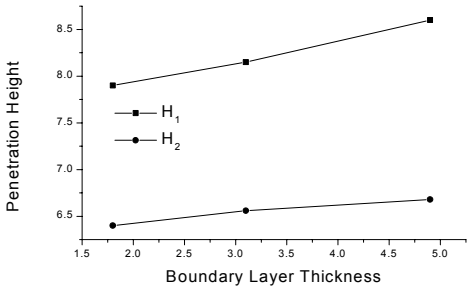

Fig. 6 Penetration height versus boundary layer thickness

Figure 5 shows the distribution of surface pressure under these boundary layer thicknesses. Penetration height and separation length versus boundary layer thickness are shown in Figs. 6 and 7. From these figures, it can be seen that the penetration height and separation length are slightly and linearly increased with the increase of the boundary layer thickness. In our study, different boundary layer thickness means different position of the injection on the 2-D plate.

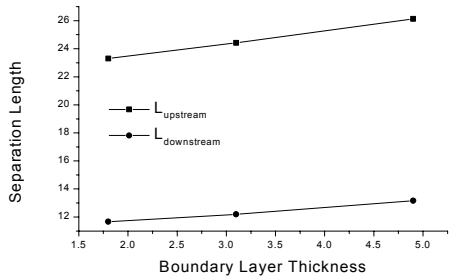

Fig. 7 Separation length versus boundary layer thickness

3.4 Width of slot nozzle

For flowfield calculation, because we use a nondimensional coordinate, which uses the width of the slot nozzle as the reference condition, the results will not change if we retain all the special conditions. But we must consider the influence of the boundary layer thickness and Reynolds number. That is, if the position of the injection is fixed, when changing the slot width, we must consider the variation of the nondimensional boundary layer thickness.

Calculation is made under the conditions of a freestream Mach number of 3.71, unit Reynolds number of $2.01\times10^7/m$, slot width of 1mm, jet Mach number of 1.0, and a total pressure ratio of 0.31. Slot widths used in our calculation are 0.5mm, 1.0mm, 1.5mm, and 2.0mm. The injection position is fixed.

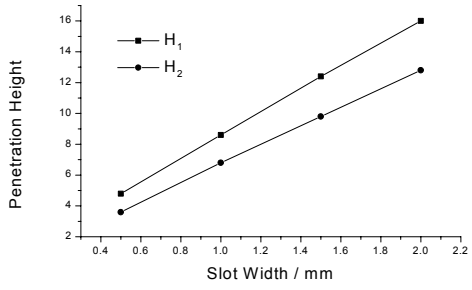

Fig. 8 Penetration height versus slot width

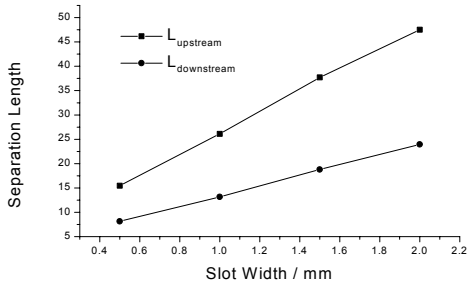

Fig. 9 Separation length versus slot width

Figures 8 and 9 show that the penetration height and separation length change almost proportionally with the slot width. For the influence of the boundary layer thickness and Reynolds number, the slopes of the lines are less 1.

3.5 Jet Mach number

The calculating condition is as follows: the freestream Mach number is 3.71, unit Reynolds number is2.01×10^7/m, slot width is 1mm, and the total pressure ratio is 0.25. The jet Mach numbers are 1.0, 1.414, 1.6, and 1.8 separately.

Figures 10 and 11 are the penetration height and separation length versus the jet Mach number. Because the total pressure of the injection is fixed, when increasing the jet Mach number, static pressure near the slot exit is decreased and both the penetration height and separation length are decreased.

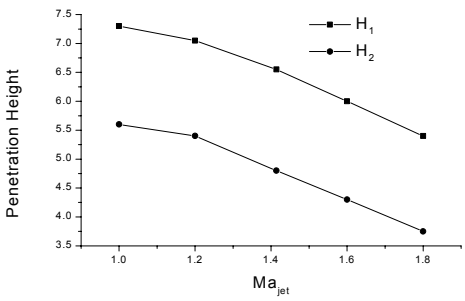

Fig. 10 Penetration height versus Mach number of injection (same slot width)

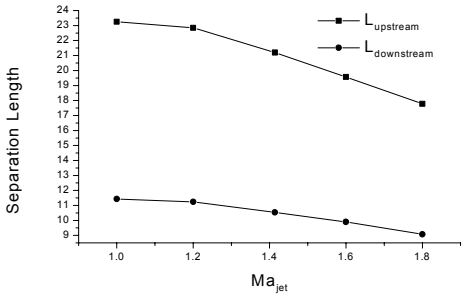

Fig.11 Separation length versus Mach number of injection (same slot width)

But in the above calculation, only the jet Mach number was considered, and the slot width is kept 1mm. That is, when increasing the jet Mach number and keeping the exit width of slot nozzle, the mass flow rate of injection is decreased. The above results are the compositive effect of Mach number and mass flow rate of the injection. For discarding the effect of the mass flow of injection, the same throat width of the injection nozzle was assumed. So the exit slot width increased according to the increase of the jet Mach number. Because the effect of boundary layer thickness was so small that it can be neglected, the separation length and penetration height change with the slot width proportionally (reference to 3.4). As a conclusion of the above discussion, Figs. 12 and 13 are obtained, which indicate that the separation length and penetration height slightly increase with the jet Mach number under a fixed mass flow rate of injection.

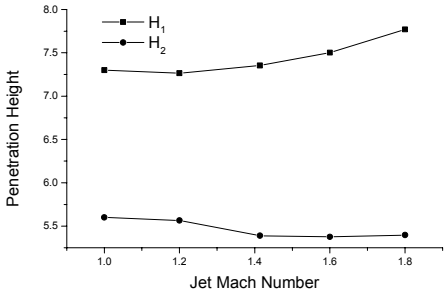

Fig.12 Penetration height versus Mach number of injection (Same flow rate of injection)

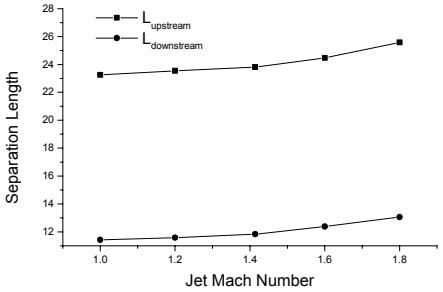

Fig.13 Separation length versus Mach number of injection (Same flow rate of injection)

3.6 Freestream Mach number

For the influence of the freestream Mach number, only two results are given. All the initial and boundary conditions are same except for the inlet condition, which one is 3.71M and the other is 2.5M. The slot width is 1mm and the total pressure ratio of jet to freestream is 0.25.

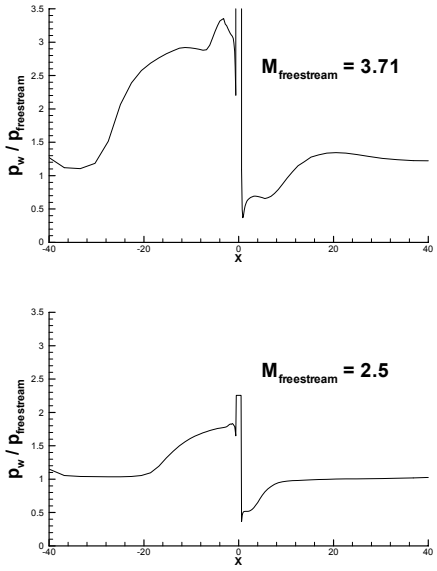

Fig. 14 Distribution of surface pressure under different Mach numbers of freestream

Figure 14 is the distribution of the surface pressure under these two Mach numbers, which indicates that the influence of the injection is weakened rapidly when the freestream Mach

number is decreased. In fact, this is the main result of the pressure ratio. Under the same stagnation parameter, when decreasing the freestream Mach number, the static pressure around the injection exit is increased, so the expansion of the jet is restricted within a small region.

3.7 Jet angle

In our study, the jet angle is defined as the angle of jet and freestream direction. When the jet and freestream are the same in direction, the jet angle is zero.

The flowfield with seven jet angles were calculated, which were 45°, 60°, 75°, 90°, 105°, 120°, and 135°. The other calculating conditions were same: the freestream Mach number is 3.71, unit Reynolds number of freestream is $2.01\times10^7/m$, slot width is 1mm, and the total pressure ratio of jet to freestream is 0.25.

The results are shown in Figure 15 and Figure 16, from which one can see that both the penetration height and separation length have peak values. When the jet angle is 105°, the two penetration heights and separation length of downstream reach their maximum while the separation length of upstream reaches its maximum when the jet angle is 120°.

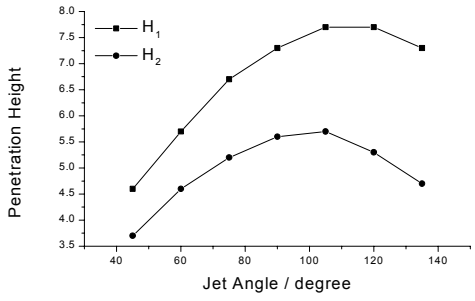

Fig.15 Penetration depth versus jet angle (same slot width)

But the same slot width under different a jet angle means a different mass flow rate of injection. Because of the same reason and method discussed in 3.5, the variation of the penetration height and separation length with the jet angle under the same flow rate of injection are obtained, which are shown in Figs. 17 and 18. Penetration height and separation length increase more and more rapidly when increasing the jet angle under the same mass flow rate of injection.

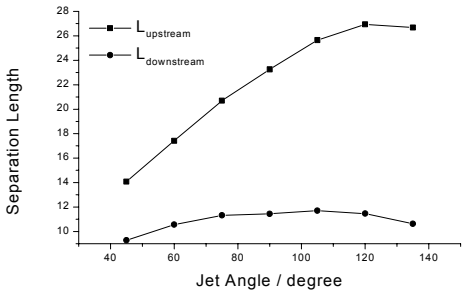

Fig.16 Separation length versus jet angle(same slot width)

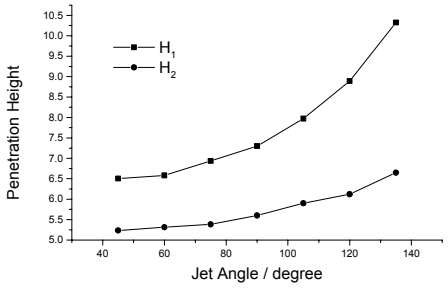

Fig.17 Penetration height versus jet angle (Same flow rate of injection)

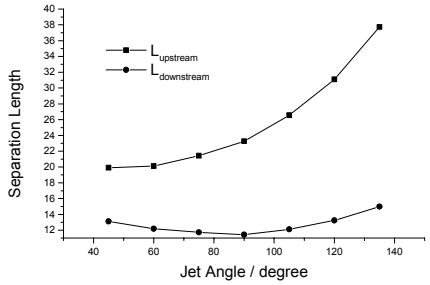

Fig.18 Separation length versus jet angle (Same flow rate of injection)

3.8 Shape of jet orifice

In 3-D flow, the orifice shape of the injection also affects the flowfield. In our study, only a rectangular shape was considered because it is

too complex to construct the mesh around the injection. The aspect ratios of the rectangles are 8:3, 3:8, and 1:1, which are marked with rec1, rec2, and squ. The areas of these rectangles are equal so as to maintain the equal jet flow rate.

Figure 19 is the distribution of the Mach number on the cross section passing through the jet center. There is no evident difference among each figure but the diffuse velocity of the injection pass rec2 is slightly faster.

Figure 20 shows the distribution of the Mach number on a symmetric section and the streamline started from the jet center is signed. When the length of the rectangle side along the freestream direction increases, the bow shock wave becomes weaker and the barrel chock wave leans to the wall, but the penetration height increases slightly.

Figure 21, the wall pressure with different jet hole orifices, clearly indicates the tendency that the upstream separation point closes up to the injection simultaneously.

4 Conclusions

Several groups of 2-D and 3-D supersonic flowfields are calculated to study the main parameters affecting the flow.

The pressure ratio of jet to freestream is the most important parameter that strongly affects the extent of the jet influence. The penetration height and separation length increase with the pressure ratio linearly. The effect of the boundary layer thickness is very small and it can be neglected. So the injection changes with the width of the slot nozzle nearly proportionally. For the same exit width of the slot nozzle, by increasing the jet Mach number, the decrease of exit pressure and the mass flow rate of the injection induce its influence. But if the jet flow rate is kept, the separation length and penetration height will slightly increase with the jet Mach number. The jet angle is also an important parameter. For the condition of the same slot width, both the penetration height and separation length have peak values. But they will increase quickly with the jet angle if the jet flow rate is kept.

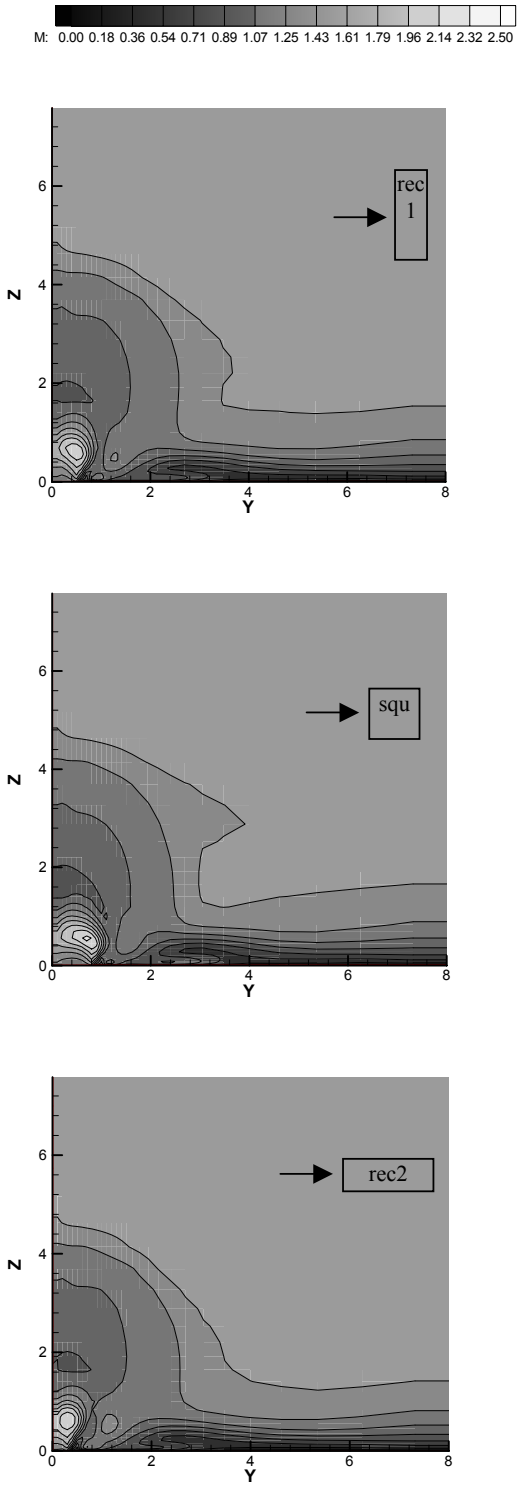

Fig. 19 Distribution of Mach number on cross section pass through jet center

The shape of the jet orifice plays a role in the 3-D flowfield but the influence is not obvious. When the length of the rectangle side along the freestream direction increases, the bow shock wave becomes weaker and the barrel chock wave leans to the wall, but the penetration height and the diffuse velocity of the jet increase slightly

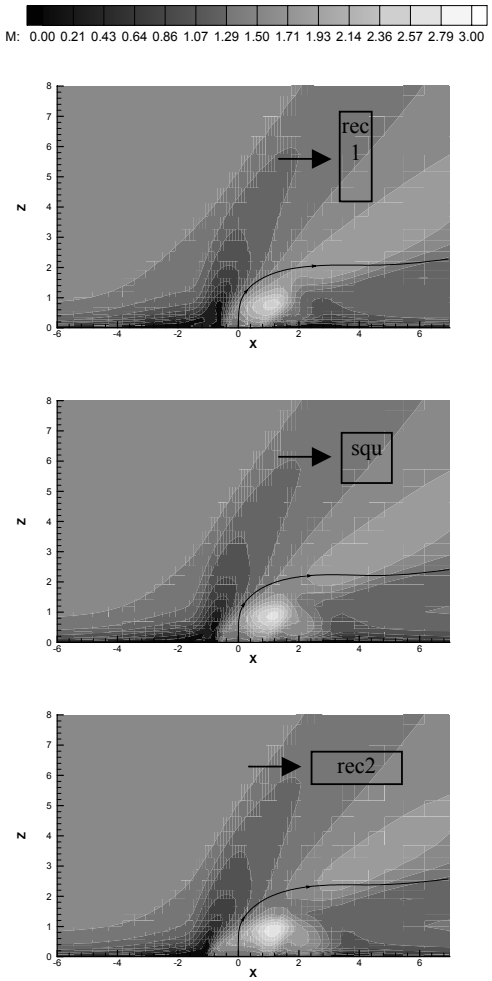

Fig. 20 Distribution of Mach number on symmetric section

References

[1] Zukoski E. E. and Spaid F. W. Secondary Injection of Gases into a Supersonic Cross Flow. AIAA Journal, 2 (10) 1964: 1689-1696.

[2] Schetz J. A. and Billig F. S. Penetration of Gaseous Jets Injected into a Supersonic Stream. Journal of Spacecraft, 3 (11), 1966: 1658-1665.

[3] Orth R. C. and Funk J. A. An Experimental and Comparative Study of Jet Penetration in Supersnic Flow. Journal of Spacecraft and Rockets, 4 (9): 1236-1242.

[4] Povinelli F. P., Povinelli L. A. and Craven C. E. Supersonic Jet Penetration (up to Mach 4) Into a Mach 2 Airstream. AIAA Journal, Vol. 9, 1971: 988-992.

[5] Cohen L. S., Coulter L. J., and Egan W. J. Penetration and Mixing of Multiple Gas Jets Subject to a Cross Flow. AIAA Journal, Vol. 9, 1971: 718-724.

[6] Strike W. T. Analysis of Aerodynamic Disturbances Generated on a Flat Plate Containing Lateral Jet Nozzles Located in a Hypersonic Stream. AEDC-TR-67-158, January 1968.

[7] Gruber M. R., Nejad A. S. and Dutton J. C. Circular and Elliptical Transverse Injection into a Supersonic Crossflow-The Role of Large-Scale Structures. AIAA 95-2150

[8] Liscinsky D. S., True B. and Holdeman J. D. Crossflow Mixing of Noncircular Jets. Journal of Propulsion and Power, 12 (2), 1996: 225-229.

[9] Roger R. P. and Chan S. C. Parameters Affecting Penetration of a Single Jet Into a Supersonic Crossflow: A CFD Study-II. AIAA 98-0425.

[10] Guang-Shan Jiang and Chi-Wang Shu. Efficient Implementation of Weighted ENO Schemes. J. Comp. Phys. 126, 1996: 202-228

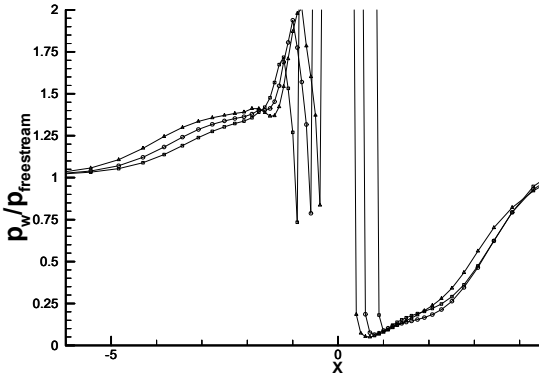

Fig. 21 Wall pressure with different jet hole orifice